



TECHNOLOGY DRIVEN. WARFIGHTER FOCUSED.

FATIGUE LIFE PREDICTION FOR ARMORED VEHICLE LAUNCHED BRIDGE (AVLB) FOR MLC 70 AND MLC 80 LOADS

16 April 2008

Bernard Sia, General Engineer

Report Documentation Page			Form Approved OMB No. 0704-0188		
Public reporting burden for the collection of information is estimated to average 1 hour per response, including the time for reviewing instructions, searching existing data sources, gathering and maintaining the data needed, and completing and reviewing the collection of information. Send comments regarding this burden estimate or any other aspect of this collection of information, including suggestions for reducing this burden, to Washington Headquarters Services, Directorate for Information Operations and Reports, 1215 Jefferson Davis Highway, Suite 1204, Arlington VA 22202-4302. Respondents should be aware that notwithstanding any other provision of law, no person shall be subject to a penalty for failing to comply with a collection of information if it does not display a currently valid OMB control number.					
1. REPORT DATE 16 APR 2008		2. REPORT TYPE N/A		3. DATES COVERED -	
4. TITLE AND SUBTITLE Fatigue Life Prediction for Armored Vehicle Launched Bridge (AVLB) for MLC 70 and MLC 80 Loads				5a. CONTRACT NUMBER	
				5b. GRANT NUMBER	
				5c. PROGRAM ELEMENT NUMBER	
6. AUTHOR(S) Bernard Sia				5d. PROJECT NUMBER	
				5e. TASK NUMBER	
				5f. WORK UNIT NUMBER	
7. PERFORMING ORGANIZATION NAME(S) AND ADDRESS(ES) US Army RDECOM-TARDEC 6501 E 11 Mile Rd Warren, MI 48397-5000				8. PERFORMING ORGANIZATION REPORT NUMBER 18828	
9. SPONSORING/MONITORING AGENCY NAME(S) AND ADDRESS(ES)				10. SPONSOR/MONITOR'S ACRONYM(S) TACOM/TARDEC	
				11. SPONSOR/MONITOR'S REPORT NUMBER(S) 18828	
12. DISTRIBUTION/AVAILABILITY STATEMENT Approved for public release, distribution unlimited					
13. SUPPLEMENTARY NOTES Paper and brief submitted for Master's class in Mechanical Engineering, University of Michigan, Dearborn MI, The original document contains color images.					
14. ABSTRACT					
15. SUBJECT TERMS					
16. SECURITY CLASSIFICATION OF:			17. LIMITATION OF ABSTRACT SAR	18. NUMBER OF PAGES 43	19a. NAME OF RESPONSIBLE PERSON
a. REPORT unclassified	b. ABSTRACT unclassified	c. THIS PAGE unclassified			

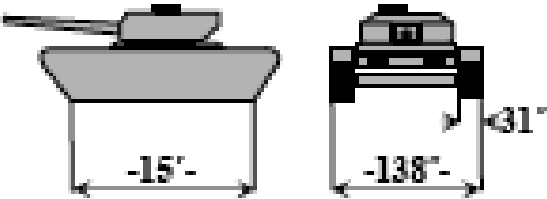

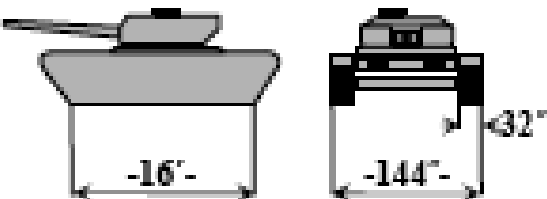

- Problem/ Task
- Background
 - Bridge Information
 - MLC
- Analysis
 - Components Analyzed
 - Assumptions and Limitations
 - Stress-Life
 - Strain-Life
 - Fracture Mechanics
- Conclusions
- Recommendations

Problem: Due to increased vehicle weight and the need to increase load carrying capacity, interest has been shown to increase the AVL B's load rating without any design changes. This may have an adverse effect on the AVL B's fatigue life.

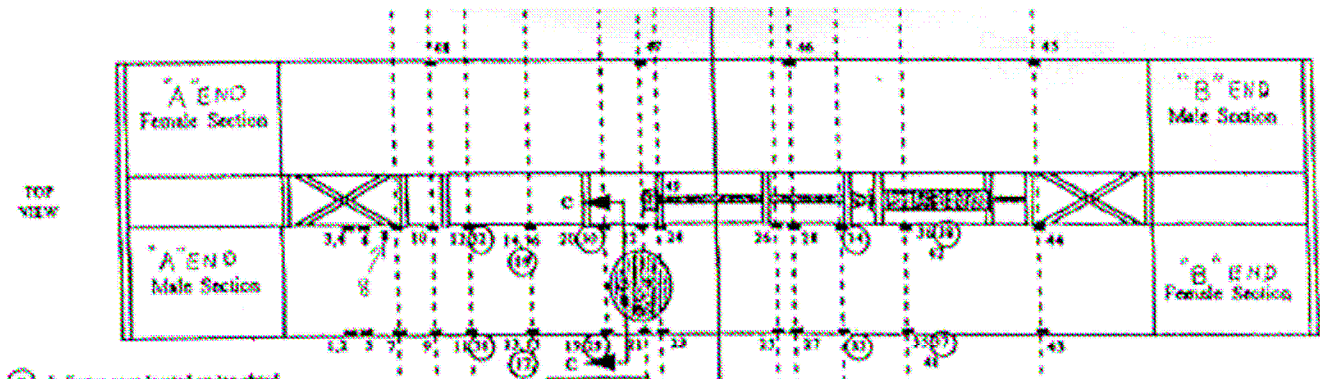
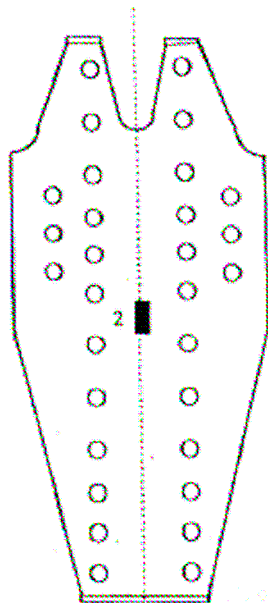
Task: To predict the fatigue life of the AVL B under MLC 70 and 80 loads

- 18.3 m (63 ft.) long
- 4 m (13 ft.) wide
- Defeats Gaps Up to 18 m (60 ft.) clear span
- Originally designed for MLC 60 loads
 - Fatigue Not Considered in Design
- MLC 70 Upgrade 1990s
 - Fatigue Life Requirement: 5000 crossings



70	<p>70.00 Tons</p> 	<p>80.50 Tons</p> <p>10.50 21.00 21.00 14.00 14.00</p> 
80	<p>80.00 Tons</p> 	<p>92.00 Tons</p> <p>12.00 24.00 24.00 16.00 16.00</p> 

Strain Gage	Material	Component
2	T-1 Steel	Splice Plate
27	7050-T76511	Bottom Chord Flange
29	2014-T6	Top Chord Flange
30	2014-T6	Top Chord Flange
31	2014-T6	Top Chord Flange
55	7050-T74	Hinge Area
56	7050-T74	Hinge Area



Stress-Life:

$$\text{Log}(N_f) = A1 + A2 * \log(S_{eq} - A4)$$

$$S_{eq} = S_{\max} (1 - R)^{A3}$$

Modified Morrow:

$$\epsilon_a = \frac{\sigma'_f}{E} \left(1 - \frac{\sigma_m}{\sigma'_f}\right) (2N_f)^b + \epsilon'_f (2N_f)^c$$

Strain-Life:

SWT:

$$\sigma_{\max} \epsilon_a = \frac{(\sigma'_f)^2}{E} (2N_f)^{2b} + \sigma'_f \epsilon'_f (2N_f)^{b+c}$$

Fracture
Mechanics:

$$\frac{da}{dN} = \frac{C \Delta K^n}{(1 - R) K_c - \Delta K}$$

$$\Delta K = F k_t \Delta S \sqrt{\pi a}$$

- Assumptions
 - Components w/ max stress < 20 ksi have no effect on fatigue life
 - Stress ratio = 0
 - Tracked vehicle effect worse than wheeled
- Limitations
 - Only considers MLC 70, MLC 80 vehicle
 - MLC 80 stresses, strains may not reflect true behavior
 - 50 % reliability and confidence only

- Strain-Life

- σ_f' = Fatigue Strength Coefficient
- ϵ_a = Strain Amplitude
- ϵ_f' = Fatigue Ductility Coefficient
- b = Fatigue Strength Exponent
- c = Fatigue Ductility Exponent
- σ_m = Mean Stress
- E = Young's Modulus
- N_f = Crossings

- Stress-Life

- $A1, A2, A3$ = Constants
- R = Stress Ratio
- $A4$ = Fatigue Limit Stress
- S_{eq} = Equivalent Stress
- S_{max} = Maximum Stress
- N_f = Crossings (Cycles)

- Fracture Mechanics

- ΔK = Change in Fracture Toughness
- C = Paris Law Coefficient
- n = Paris Law Exponent
- a_c = Final Crack Length
- a_i = Initial Crack Length
- σ_o = Yield Stress
- K_{Ic} = Critical Fracture Toughness
- F = constant based on geometry, loading case, and ratio of crack length and dimensions of the component or test specimen
- k_t = Stress Concentration Factor

Strain Gage	Material	# of Cycles		% Change
		MLC 70	MLC 80	
2	T-1 Steel	9.86E+08	5.42E+08	45.0
27	7050-T76511	2.24E+07	5.24E+06	76.7
29	2014-T6	2.30E+06	6.17E+05	73.2
30	2014-T6	1.54E+08	4.10E+07	73.4
31	2014-T6	4.10E+05	1.08E+05	73.6
55	7050-T74	3.62E+04	1.74E+04	52.0
56	7050-T74	1.95E+04	9.78E+03	49.9
	Overall Life	1.95E+04	9.78E+03	

Strain Gage	Material	Cycles			Cycles		
		(Morrow)			(SWT)		
		MLC	MLC	%	MLC	MLC	%
		70	80	Change	70	80	Change
2	T-1 Steel	6.08E+11	1.13E+11	81.4	2.98E+10	7.11E+08	97.6
27	7050-T76511	1.01E+10	1.94E+09	80.8	5.20E+08	1.17E+08	77.5
29	2014-T6	6.91E+07	2.95E+07	57.2	n/a	n/a	n/a
30	2014-T6	2.75E+09	8.76E+08	68.1	n/a	n/a	n/a
31	2014-T6	2.15E+07	7.36E+06	65.8	n/a	n/a	n/a
55	7050-T74	6.52E+05	1.10E+05	83.1	1.76E+05	4.18E+04	76.3
56	7050-T74	1.78E+05	3.10E+04	82.5	6.33E+04	1.56E+04	75.4
	Total Life (crossings)	1.78E+05	3.10E+04		6.33E+04	1.56E+04	

Strain Gage	Crack Length (m)							
	0.0001		0.0005		0.001		0.002	
	MLC 70	MLC 80	MLC 70	MLC 80	MLC 70	MLC 80	MLC 70	MLC 80
2	4.9E+18	3.3E+18	2.7E+18	1.8E+18	2.0E+18	1.3E+18	1.4E+18	8.5E+17
27	2.3E+05	1.7E+05	9.0E+04	6.2E+04	5.0E+04	3.2E+04	1.8E+04	7.6E+03
29	4.0E+04	2.2E+04	n/a	n/a	n/a	n/a	n/a	n/a
30	1.5E+05	1.0E+05	2.0E+04	5.5E+03	n/a	n/a	n/a	n/a
31	1.3E+04	5.7E+03	n/a	n/a	n/a	n/a	n/a	n/a
55	2.4E+04	1.5E+04	3.6E+03	7.1E+02	n/a	n/a	n/a	n/a
56	1.7E+04	1.0E+04	1.4E+03	n/a	n/a	n/a	n/a	n/a

- The AVLB should be able to satisfy the fatigue life requirement of 5000 crossings for both MLC 70 and 80 crossings.
- Overall percent change in fatigue life ranges from 50-80 percent.
- The stress-life approach provides a more conservative estimate of the bridge's life than does the strain-life approach.
- Hinge, Top Chord are critical parts in determining AVLB fatigue life
- Depending on the critical crack size of the component, a fracture analysis may be a more or less conservative estimate of fatigue life for the AVLB.
- Cracks have more adverse effect on Top Chord, Hinge than Splice Plate, Bottom Chord
- Top Chord, Hinge more dependent on initial crack size than Splice Plate, Bottom Chord

- Test the AVLB to qualify it at MLC 80
- Refine the estimate to reflect 95 percent reliability and confidence (R95C95).
- Verify the results of the analysis.

**FATIGUE LIFE PREDICTION FOR ARMORED VEHICLE LAUNCHED BRIDGE
(AVLB) FOR MLC 70 AND MLC 80 LOADS**

Bernard Sia
General Engineer, US Army TACOM

ME 558 Project
University of Michigan – Dearborn
April 9, 2008

UNCLASSIFIED: Dis. A. Approved for public release

Symbols

R = Stress Ratio
r = Load Ratio
 N_f = Cycles (Crossings)
E = Young's Modulus
P = Applied Load
 W_{veh} = Vehicle Weight
DF = Dynamic Factor
 E_{cc}/S_s = Eccentricity/ Side Slope Factor
 W_{mud} = Mud Load
ULF = Uniform Load Factor

Stress-Life

- A_1, A_2, A_3 = Constant
- A_4 = Fatigue Limit Stress
- S_{eq} = Equivalent Stress
- S_{max} = Maximum Stress

Strain-Life

- σ_f' = Fatigue Strength Coefficient
- ϵ_a = Strain Amplitude
- ϵ_f' = Fatigue Ductility Coefficient
- b = Fatigue Strength Exponent
- c = Fatigue Ductility Exponent
- σ_m = Mean Stress

Fracture Mechanics

- ΔK = Change in Fracture Toughness
- C = Paris Law Coefficient
- n = Paris Law Exponent
- a_c = Final Crack Length
- a_i = Initial Crack Length
- σ_o = Yield Stress
- K_c = Critical Fracture Toughness
- F = constant based on geometry, loading case, and ratio of crack length and dimensions of the component or test specimen.
- k_t = Stress Concentration Factor

ABSTRACT

An analysis was performed to predict the fatigue life of the Armored Vehicle Launched Bridge (AVLB) for Military Load Class (MLC) 70 and 80 loads. Fatigue life was estimated using stress-life, strain-life, and fracture mechanics approaches. The analysis was focused on 4 different components, as these components showed the highest stress magnitude during MLC 70 testing. The stress-life approach provided the most conservative estimate of fatigue life. All three approaches predicted that the bridge will satisfy the Army Engineer School's durability requirements under both loads. Stress-life provided the most conservative fatigue life estimate. The percent change in the bridge's fatigue life varied with analysis approach. Further testing will be required to validate the results of the analysis.

Keywords: AVLB, Fatigue Life, Stress-Life, Strain-Life, Fracture

1. INTRODUCTION

In response to the current war in Iraq, the United States Army and its contractors have developed many new technologies for their vehicles. This technology has helped to improve their lethality and survivability, as well as increase the level of protection for the soldiers. However, this new technology has also resulted in an increase in weight. This increase in weight may have an adverse effect on its ability to defeat natural and man-made obstacles.

Gaps are one of these obstacles. The Army has various gap defeat equipment to defeat various mission, including assault and line of communication. One of the gap defeat equipment is the Armored Vehicle Launched Bridge (AVLB), an assault bridge in service since the 1960s. Upgrades to the bridge have increased its carrying capacity from a Military Load Class (MLC) 60 to MLC 70. Test results for the bridge have shown greater load carrying capacity than its load rating. Because of this, interest has been shown in increasing the load rating of the bridge without making any further design changes to the bridge. While increasing the rating of the bridge is desired, it may have an adverse effect on its durable life.

The purpose of this report is to present the fatigue life prediction for the AVLB under MLC 70 and MLC 80 loads. The calculations were performed using stress-life, strain-life, and fracture mechanics methods. This report presents the results and conclusions of the analyses.

2. BACKGROUND

2.1 AVLB

The AVLB, shown in Figure 1, is a scissor-launched girder bridge used by the US Army to defeat gaps with a clear span of up to 18 meters (60 feet) long. Introduced to the US Army in the 1960s, it has an overall length and width of 63 feet (18.3 m). Its total width is 13 feet (4.0 m). It is constructed using aluminum alloys and hot rivets. The bridge, introduced to support the M48 and M60 Tank, was originally designed to carry loads up to MLC 60. The bridge design did not

consider fatigue life. The bridge rides atop and is hydraulically launched by either an M48 or M60 chassis. Bridge launch time is 5 minutes, while retrieval time is 10 minutes.



Figure 1: AVLB On Top of Launch Vehicle

Due to increasing vehicle weights and the need for a bridge to support the M1 Abrams, the AVLB was upgraded to MLC 70 in the 1990s. At this stage, fatigue became an important consideration due to a requirement set forth by the Army Engineer School that the bridge be able to sustain 5000 MLC 70 crossings. Changes were incorporated to the bridge to meet the fatigue life requirement. The bridge's structural center hinge and bottom chord was now manufactured from 7050 aluminum alloy instead of 2014 aluminum alloy. The bottom chord was also made continuous from the ramp to the center section. Previously, these two sections were pinned together. Some fasteners were also changed from hot rivets to huck bolts.

Fatigue calculations were performed to analyze the life of the bridge for MLC 60 and MLC 70 loads. The calculations performed were mainly stress-based, but strain-life was also considered. These calculations were performed to estimate the change in fatigue life due to the life of the bridge. However, the total fatigue life of the bridge was never determined. Durability testing had been performed on the bridge for the 5000 crossing requirement. No durability testing to qualify the bridge for more than 5000 crossings was performed.

The changes made to the bridge also improved the overall capacity of the bridge. It not only survived under MLC 70 loadings, but also showed a possibility of higher capacity, as its failure load was much higher than the bridge's rating. It is this possibility of higher capacity, along with the continued increasing of vehicle weight due to add-ons, that created the need to look at increasing the rating of the bridge.

2.2 MLC

A discussion of the Military Load Class (MLC) is required, as it determines that loads at which the analysis is performed. The MLC is a number that is applicable to both the vehicles and bridges. The MLC represents the load rating of the vehicle, as well as the design capacity of the bridge. The vehicle rating is compared with the design capacity to determine whether the vehicle can safely cross the bridge.

The calculation of MLC for a vehicle is dependent on the weight of the vehicle. However, the vehicle's footprint can also influence the rating. A more compact footprint will have a worse effect on a structure than a larger footprint with the same weight. The first step of the calculation is to determine the maximum bending moments and shear forces induced by the vehicle over spans of up to 300 feet (100 m). Using these values, the vehicle's rating is then determined by interpolation among tables of standardized bending moments and shear forces. The standardized bending moments and shear forces are based on a set of standardized tracked and wheeled vehicles, known as hypothetical vehicles. Corrections are then made to the vehicle's rating depending on geometrical factors, such as the difference in the width of the vehicle with that of the hypothetical vehicle. Figure 2 shows the hypothetical vehicles representative of the current rating and potential rating of the AVLB.

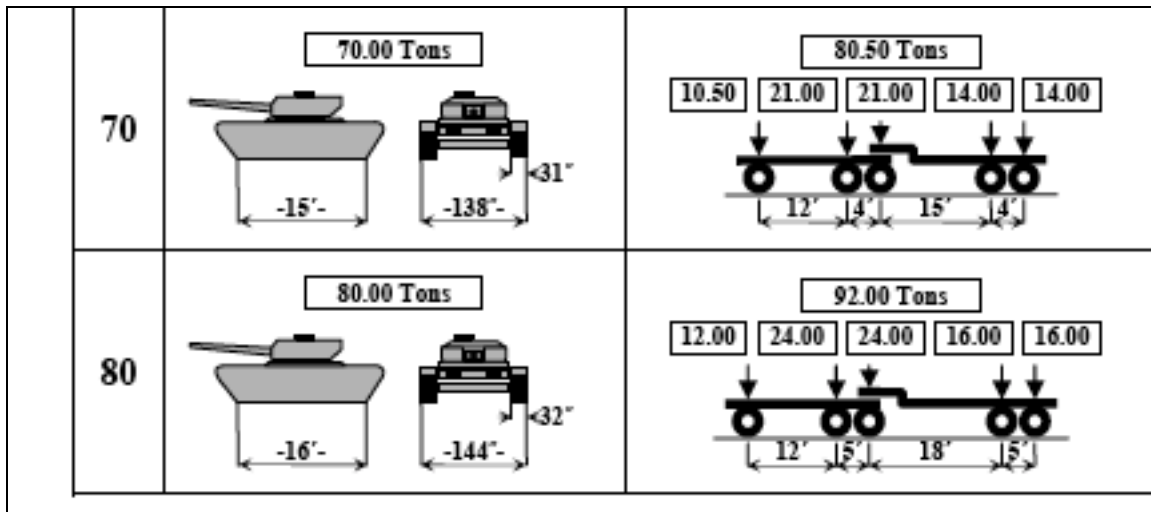


Figure 2: Hypothetical MLC 70 and 80 Vehicle (US Units)

The U.S. Army establishes the MLC of each bridge. The MLC is dependent mainly on the vehicles that the bridge will be designed to sustain. Once the bridge has been designed, it then undergoes three tests to qualify the bridge for the MLC and span:

- Working Load: the load (vehicle load + dynamic factors) that the bridge will carry;
- Overload: the bridge's working load multiplied by a safety factor of 1.33
- Ultimate Load: the bridge's working load multiplied by a safety factor of 1.5

3 METHODOLOGY

3.1 Assumptions and Limitations

Many assumptions were made to simplify the analysis. It was assumed that components whose maximum stress over the course of overload testing did not exceed 20 ksi would have no effect on fatigue life. Correlating the material S-N curves with these stresses resulted in fatigue lives on the order of at least 10^8 cycles. Damage, equal to inverse of the number of cycles, is negligible for such high cycle amounts. A stress ratio, equal to $\sigma_{\min}/\sigma_{\max}$, of 0 was also assumed. Traditionally the bridge is fully unloaded at the end of a test run. Tracked vehicles were

assumed to have a worse effect on the bridge than wheeled vehicles due to its weight being comprised in a more compact footprint.

The analysis also has its limitations. The analysis only considers crossings by a pure MLC 70 and MLC 80 tracked vehicle. It does not consider effects due to crossings of vehicles whose MLC differs from that of the bridge's rating. This was done because the true usage of this bridge, such as what vehicles cross and what frequency, is unknown. The analysis does not consider effects to the bridge due to its cantilever method of launching. The MLC 80 data was estimated by assuming linearity. The stresses and strains produced by this assumption may not accurately represent the actual effect of the MLC 80 load on the AVLB. Finally, due to insufficient statistical data, the lives calculated in this analysis reflect 50 percent reliability and confidence. Some statistical data on the various properties will be needed to convert the data to reflect 95 percent reliability and confidence as specified in [1].

3.2 Stress-Strain Data

The stress and strain data used for this analysis was generated during static testing of the MLC 70 design. A total of 51 strain gages and 6 strain rosettes were used to collect data during this testing. Loads were applied at $\frac{1}{2}$ and $\frac{1}{4}$ of the bridge's clear span, equal to 60 feet (18 m). Table 1 lists the loads applied to the bridge during this testing. All loads were calculated using 70 tons as its vehicle load, as well as constants used to estimate dynamic effects on the bridge.

Test	Applied Load, 1/2 Span Tests (tons/ kg)	Applied Load, 1/4 Span Tests (tons/ kg)
Working Load	95/ 86,200	n/a
Overload	129/ 117,000	139/ 126,100
Ultimate Load	147/ 133, 400	158/ 143,300

Table 1: Applied Loads for AVLB MLC 70 Testing

Working load data was used in this analysis as the stresses and strains produced by the working load are more representative of those seen during usage of the bridge. Because test data was only collected for overload and ultimate load testing, the data needed to be converted to reflect

working load conditions. Assuming linearity, the data was converted to working load values by multiplying the data by the following ratios:

$$r_{Overload} = \frac{P_{workingload}}{P_{overload}} \quad (1)$$

$$r_{Ult.Load} = \frac{P_{workingload}}{P_{Ult.Load}} \quad (2)$$

Because working load testing is only performed at $\frac{1}{2}$ span, a “working load” for $\frac{1}{4}$ span, equal to 102 tons (92,500 kg), was calculated using Equation (3).

$$P_{WL} = [(W_{veh} * D_f * \frac{E_{cc}}{S_s}) + W_{mud} * ULF] \quad (3)$$

Test data from the MLC 70 upgrade was also used to provide an estimate of the stresses and strains expected during an MLC 80 crossing of the AVLB. All MLC 70 data was scaled up by 8/7, the ratio of the weight of the MLC 80 hypothetical vehicle in tons and the MLC 70 hypothetical vehicle weight in tons. This was done because the AVLB showed no signs of nonlinearity during MLC 70 testing. Estimation of MLC 80 stresses and strains was necessary because testing of the AVLB has not been performed under MLC 80 loads as yet. Once the bridge is tested for MLC 80, the data can be used to produce a better fatigue estimate for the AVLB at MLC 80.

Using the assumption that stress levels below 20 ksi (138 MPa) will not affect fatigue life, the focus of the analysis was narrowed down to data from 7 strain gages. These gages were located on components that saw the highest stresses and strains during testing. Table 2 lists these gages with the component it is attached to and material from which the component is manufactured. Figures which show the location of each gage on the bridge can be found in Appendix A.

Strain Gage	Material	Component
2	T-1 Steel	Splice Plate
27	7050-T76511	Bottom Chord Flange
29	2014-T6	Top Chord Flange
30	2014-T6	Top Chord Flange
31	2014-T6	Top Chord Flange
55	7050-T74	Hinge Area
56	7050-T74	Hinge Area

Table 2: Areas of Focus for Fatigue Analysis of AVLB

3.3 Stress-Life

A stress-based approach was used to provide an initial estimate for the fatigue life of the AVLB. This approach had been used during the MLC 70 upgrade to predict the percent improvement of component fatigue life resulting from the changes to the bridge. It uses stress-life curves, or S-N curves, to determine life of a component. This approach assumes that cyclic stresses are the main cause of fatigue failure. For this analysis, S-N curves developed in the Metallic Material Properties Development and Standardization (MMPDS) Handbook were used to calculate the fatigue life of each aluminum components. The S-N curves developed in the handbook were based on an equivalent stress approach, which considers the stress ratio using the following equation:

$$S_{eq} = S_{max} (1 - R)^{.43} \quad (4)$$

In this approach, the equation for the best-fit line representing the S-N curve of the material assumes the following form:

$$\text{Log}(N_f) = A1 + A2 * \log(S_{eq} - A4) \quad (5)$$

For compressive stresses, the absolute value of S_{eq} was used to perform the calculation. If $A4$ is equal to 0, the equation reduces to

$$\text{Log}(N_f) = A1 + A2 * \log(S_{eq}) \quad (6)$$

The S-N curve of T-1 Steel was estimated based on its ultimate tensile strength, since an applicable S-N model for the material could not be found. The procedure for this estimate is presented in Lee [4]. The calculation of this S-N curve can be found in Appendix B. Once S-N curves were used to relate maximum stress to the number of cycles, damage was estimated using the equation

$$\text{Damage} = d = \frac{1}{N_f} \quad (7)$$

Overall fatigue life of each component was then calculated using the equation

$$\text{Life} = \frac{1}{\sum d_i} \quad (8)$$

3.4 Strain-Life

A strain-based approach, having some similarities to the stress-based approach, was used to provide a second estimate. This approach uses a strain-versus-life plot to model the fatigue life of a component due to various strain levels. Two models were used for strain-life estimate: the modified Morrow model, which expresses the strain-life relationship as

$$\varepsilon_a = \frac{\sigma'_f}{E} \left(1 - \frac{\sigma'_m}{\sigma'_f}\right) (2N_f)^b + \varepsilon'_f (2N_f)^c \quad (9)$$

and the Smith-Watson-Topper (SWT) model, which expresses strain-life as

$$\sigma_{\max} \varepsilon_a = \frac{(\sigma'_f)^2}{E} (2N_f)^{2b} + \sigma'_f \varepsilon'_f (2N_f)^{b+c} \quad (10)$$

Both models take mean stress and plastic strains into account. Due to insufficient data, all strain-life constants, with the exception of 2014-T6, were estimated using the procedure developed by Baumel and Seeger, as given in [4]. Strain-life constants used for 2014-T6 were obtained in SAE J1099. [5]. Table 3 shows the values of each constant used in this analysis for each material.

Material	E (ksi/ MPa)	σ'_f (ksi/ MPa)	ε'_f	b	c
2014-T6	10,000/ 69,000	146/ 1008	1.418	-0.114	-0.87
7050-T76511	10,200/ 70,300	110/ 760	0.35	-0.095	-0.69
7050-T74	10,200/ 70,300	110/ 760	0.35	-0.095	-0.69
T-1 Steel	30,500/ 210,000	194/ 1336	0.53	-0.087	-0.69

Table 3: Strain-Life Constants for Materials Comprising AVL B

Damage was calculated by taking the inverse of each N_f value obtained from the Morrow and SWT model. The total life was then calculated by taking the inverse of the sum of all damage resulting from the tests.

3.5 Fracture Mechanics

A fatigue crack analysis was also performed to predict the fatigue life of the bridge with a crack present. The purpose of this calculation was to determine how large of a crack can be tolerated by the bridge before its fatigue life falls below 5000 crossings. Prior to performing the fracture

calculation, the following check, as presented in Dowling [6] was made to confirm the applicability of Linear Elastic Fracture Mechanics (LEFM) for the component:

$$a, (b-a), h \geq \frac{4}{\pi} \left(\frac{K}{\sigma_o} \right)^2 \quad (11)$$

If the component passed the criteria presented in Equation 11, a model similar to that used by Choi [7] was used to provide a fracture-based fatigue estimate. According to LEFM, a change in fracture toughness of a material can be expressed as

$$\Delta K = F k_t \Delta S \sqrt{\pi a} \quad (12)$$

Stress concentrations were taken into account by using the constant k_t . To simulate the effect of the rivet holes on the bridge, each component was modeled as a remotely loaded wide plate with a circular hole. For this specimen, F is assumed to be 1.12. Each component was assumed to be made of an isotropic material; therefore, k_t equals 3 for this case [9].

Paris Law was used to represent the crack growth behavior of each material. Paris Law is expressed as

$$\frac{da}{dN} = C(\Delta K)^n \quad (13)$$

Integration of this equation results in an expression for fatigue life as a function of initial and final crack length. For this analysis, the following expression, as presented in Dowling [6], was used:

$$N_{if} = \frac{a_f^{1-n/2} - a_i^{1-n/2}}{C(F\Delta S\sqrt{\pi})^n (1-n/2)} \quad (14)$$

This expression assumes that C , F , ΔS , and m are constant for each component. Equation 14 is highly dependent on the initial crack length, as most of the cycles are accumulated around this crack length. Because of this dependence, various initial crack lengths were considered.

The final crack length, a_c , was calculated using the following formula

$$a_c = \frac{1}{\pi} \left(\frac{K_{Ic}}{1.12k_t \sigma_{\max}} \right)^2 \quad (15)$$

Table 4 lists the final crack lengths calculated for each strain gage considered in the analysis, as based on the maximum stress level experienced by the component during bridge testing.

Strain Gage	a_c MLC 70 (mm)	a_c MLC 70 (in)	a_c MLC 80 (mm)	a_c MLC 70 (in)
2	21	0.813	16	0.612
27	3.2	0.124	2.6	0.100
29	0.34	0.0132	0.25	0.01
30	0.69	0.0273	0.56	0.0221
31	0.20	0.008	0.15	0.006
55	0.74	0.029	0.55	0.0218
56	0.60	0.0238	0.45	0.0179

Table 4: Critical Crack Lengths for Each Strain Gage, As Based on the Maximum Stress

If the component could not be modeled using LEFM, an equation developed by Forman, Kearney, and Engle was used. This equation takes nonlinear crack growth rate- ΔK plots into account by using the R-ratio. This equation has various forms; the model of the equation used in this analysis is shown below.

$$\frac{da}{dN} = \frac{C \Delta K^n}{(1-R)K_c - \Delta K} \quad (16)$$

4. RESULTS

4.1 Stress-Life

Table 5 shows the results of the analysis, using the stress-life approach. The number of cycles listed in Table 5 represent the minimum number of crossings that can be run at the stresses created by an MLC 70 and MLC 80 loading.

Strain Gage	Material	# of Cycles		
		MLC 70	MLC 80	% Change
2	T-1 Steel	9.86E+08	5.42E+08	45.0
27	7050-T76511	2.24E+07	5.24E+06	76.7
29	2014-T6	2.30E+06	6.17E+05	73.2
30	2014-T6	1.54E+08	4.10E+07	73.4
31	2014-T6	4.10E+05	1.08E+05	73.6
55	7050-T74	3.62E+04	1.74E+04	52.0
56	7050-T74	1.95E+04	9.78E+03	49.9
	Overall Life	1.95E+04	9.78E+03	

Table 5: Component Life reduces by approximately 50-75% by increasing to MLC 80 Loads

The analysis shows that the life of each component reduces by about 50 to 74 percent by increasing the capacity of the bridge from MLC 70 to MLC 80. However, all components exceed the durability requirement of 5000 crossings specified by the Engineer School. The total predicted number of MLC 70 and MLC 80 crossings across the AVL B is approximately 19,500 and 9800 crossings, respectively. The overall life of the bridge is governed by the results of gage 56, located at the hinge. The stresses seen by this gage were higher than that experienced by any other gage. This resulted in the lowest number of cycles of any component considered in the analysis.

4.2 Strain-Life

The results of the strain-life approach, using both models, are shown in Table 6.

Strain Gage	Material	Cycles (Morrow)			Cycles (SWT)		
		MLC 70	MLC 80	% Change	MLC 70	MLC 80	% Change
2	T-1 Steel	6.08E+11	1.13E+11	81.4	2.98E+10	7.11E+08	97.6
27	7050- T76511	1.01E+10	1.94E+09	80.8	5.20E+08	1.17E+08	77.5
29	2014-T6	6.91E+07	2.95E+07	57.2	n/a	n/a	n/a
30	2014-T6	2.75E+09	8.76E+08	68.1	n/a	n/a	n/a
31	2014-T6	2.15E+07	7.36E+06	65.8	n/a	n/a	n/a
55	7050-T74	6.52E+05	1.10E+05	83.1	1.76E+05	4.18E+04	76.3
56	7050-T74	1.78E+05	3.10E+04	82.5	6.33E+04	1.56E+04	75.4
	Total Life (crossings)	1.78E+05	3.10E+04		6.33E+04	1.56E+04	

Table 6: SWT model predicts lower fatigue life for AVLB than Morrow.

Overall, SWT provided a more conservative estimate of fatigue life of the bridge than the Modified Morrow model. SWT predicts a fatigue life of approximately 63,000 and 16,000 crossings for MLC 70 and 80, respectively, compared to 180,000 and 31,000 crossings for Morrow. While the Morrow model could predict fatigue life for all gages, SWT could only calculate life for four of the gages. SWT had problems with the compressive strains and corresponding stresses that were read by gages 29, 30, and 31. SWT uses zero as its σ_{\max} when the loading is purely compressive. Because SWT never converges to zero, a cycle value cannot be obtained for these gages.

Differences also exist in the percent change in fatigue life due to increasing the bridge capacity from MLC 70 to MLC 80. With the exception of the top chord (gages 29, 30, and 31), the

Morrow model predicts a reduction in component fatigue life of 80-83 percent. For the top chord, Morrow shows a reduction of between 57 to 68 percent. SWT shows a more consistent reduction in life among materials. The hinge and splice plate, made respectively out of 7050 Aluminum and T-1 Steel, show a reduction of life between 75 and 98 percent.

Both models predict that the bridge will be able to fulfill the 5000 crossing requirement set by the Engineer School, regardless of the bridge's capacity. The hinge area was the component with the lowest number of crossings in both models.

4.3 Fracture Mechanics

A Fracture Mechanics analysis was performed to examine how the presence of a crack affects the life of the bridge. The fracture analysis was performed using initial crack lengths of 0.1, 0.5, 1, and 2 mm. The choice of these values was based on the critical crack lengths presented in Table 4, as most of the components had critical crack lengths lower than 2 mm. It is unknown what crack sizes are seen on the AVLB during regular service.

Using Equation 11, it was determined that LEFM was not valid for any of the components considered in this analysis. The calculated critical crack size for all components was lower than that allowed by Equation 11. Because of this, Equation 16 was used. The results of this analysis for various crack lengths are shown in Table 7.

Strain Gage	Crack Length (m)							
	0.0001		0.0005		0.001		0.002	
	MLC 70	MLC 80	MLC 70	MLC 80	MLC 70	MLC 80	MLC 70	MLC 80
2	4.9E+18	3.3E+18	2.7E+18	1.8E+18	2.0E+18	1.3E+18	1.4E+18	8.5E+17
27	2.3E+05	1.7E+05	9.0E+04	6.2E+04	5.0E+04	3.2E+04	1.8E+04	7.6E+03
29	4.0E+04	2.2E+04	n/a	n/a	n/a	n/a	n/a	n/a
30	1.5E+05	1.0E+05	2.0E+04	5.5E+03	n/a	n/a	n/a	n/a
31	1.3E+04	5.7E+03	n/a	n/a	n/a	n/a	n/a	n/a
55	2.4E+04	1.5E+04	3.6E+03	7.1E+02	n/a	n/a	n/a	n/a
56	1.7E+04	1.0E+04	1.4E+03	n/a	n/a	n/a	n/a	n/a

Table 7: Hinge, Top Chord Life is Significantly Affected by Presence of Cracks

The analysis indicates that the Bottom Chord and Splice Plate are able to withstand a significant number of crossings after a crack has started to propagate. Under all initial crack lengths used in the analysis, these two components are able to last for more crossings than the bridge's specified durability requirement of 5000 crossings. However, the life of the Top Chord (Gages 29, 30, and 31) and Hinge (Gage 55 and 56) are greatly affected by the presence of a crack. The Top Chord fails at a crack length of only 0.5 mm. The hinges fail due to crack sizes greater than 0.5 mm.

Table 8 shows the magnitude of the change in cycle life due to the increased capacity. Generally, the change in component life increased with higher initial crack lengths.

	Initial Crack Length (m)			
	1.00E-04	5.00E-04	1.00E-03	2.00E-03
Strain Gage	% Change	% Change	% Change	% Change
2	31.4	32.9	34.4	37.2
27	27.7	31.2	36.3	58.2
29	44.6	n/a	n/a	n/a
30	30.6	72.5	n/a	n/a
31	56.6	n/a	n/a	n/a
55	38.5	80.5	n/a	n/a
56	39.5	n/a	n/a	n/a

Table 8: Percent Change in Component Life due to Increased Capacity

5. DISCUSSION

Based on the stress-life and strain-life analysis, the AVL B will easily meet the 5000 crossing requirement for both MLC 70 and MLC 80 loads. The bridge appears to have been designed with a high enough factor of safety that, while the number of crossings reduce when loaded at MLC 80, the bridge is still able to easily satisfy the durability requirement.

Compared to the strain-life models, stress-life gives a more conservative estimate of the fatigue life. Its estimate of component fatigue life is lower than that obtained from Morrow and from SWT. This difference is substantial for the Splice Plate, Bottom Chord Flange, and Top Chord Flange. The strain-life estimates for these components differ from the stress-life estimate by a magnitude range of 10^2 - 10^4 . The difference between stress-life and strain-life estimates for the hinge is lower, as the estimates differ by a magnitude of about 10^1 . Because the stress-life theorem gives a more conservative estimate, it seems to indicate that the life of the bridge under both MLC 70 and MLC 80 loads is governed more by the stress-life approach. These results agree with the behavior of the bridge during the Overload and Ultimate Load tests under MLC 70 loads. The Splice Plate, Bottom Chord and Top Chord Flange showed no signs of plasticity during these tests. The hinges did show some signs of plasticity during these tests. However, the

stress on the hinges never reached the yield stress over the course of these tests. Because of this, the plastic strain would not be high enough for strain-life approaches to govern. It is unknown how well this analysis will corroborate with the bridge's behavior under MLC 80 loads. The AVLB will need to be tested for MLC 80 loading.

The two approaches also differ with respect to the percent change in number of crossings. In general, the strain-life approach predicts a larger percent change for the hinge, bottom chord flange, and splice plate than does stress-life. The strain-life approach seemed to be more sensitive to changes in the applied load. As a result, a higher decrease in fatigue life resulted from an increase to MLC 80 loads. The Morrow model appeared to be more sensitive to load changes than did SWT. Stress-life, however, predicts a larger percent change for the top chord than does strain-life, possibly due to the increase in the σ_f effect by the compressive loads.

Based on the fracture analysis, the Bottom Chord and Splice Plate will be able to withstand a high number of crossings for all initial crack lengths considered in the analysis. The stresses on these components are not high enough to cause rapid crack growth. The analysis also indicates that the stress level on the Top Chord and Hinge is much too high for it to be able to sustain any damage. Neither component was able to carry MLC 70 and 80 loads when a crack larger than 0.5 mm was present. Inspections on the bridge will need to focus on these two components to ensure that any damage is detected early on. Extra design work may also be necessary to reduce the stresses on these components.

The fracture analysis showed a high dependence on the initial crack length. This dependence was greater for the Top Chord and Hinge than the Bottom Chord and Splice Plate. Changes to component life and, subsequently, the percent change in life due to the higher load became more substantial with higher initial crack lengths. This is caused by the increased stresses placed on the bridge due to the MLC 80 load. These higher stresses will result in a lower critical crack length than that seen under MLC 70 loads. Therefore, a large crack under MLC 80 loads will have a more significant effect on the life of the bridge than it would under MLC 70 loads. The dependence on the initial crack length also has an effect on the conservatism of the fatigue life estimate. In general, the fracture analysis provided a more conservative estimate of fatigue life

for each component. This is likely due to the small critical crack sizes observed. The exception to this was the splice plate, which had a critical crack length much higher than that for any other component. The fracture analysis resulted in the least conservative estimate of fatigue life for the component.

Overall, the results of this analysis provide a first estimate of the number of crossings that may be expected under both MLC 70 and MLC 80 loads. This analysis was performed with no prior knowledge of what approach actually governs the behavior of the bridge, as well as with estimated stresses and strains due to MLC 80 loadings. The results of this analysis will need to be validated by testing of actual hardware before it can be considered to be representative of the bridge.

6. CONCLUSIONS

Based on this analysis, the following conclusions are made:

- The AVLB should be able to satisfy the durability requirement of 5000 crossings under both MLC 70 and 80 crossings.
- The overall percent change in fatigue life by increasing capacity from MLC 70 to MLC 80 depended on the model used and ranges from 50-80 percent.
- The stress-life approach provides a more conservative estimate of the bridge's life than does the strain-life approach.
- The Hinge and Top Chord are more critical than the Bottom Chord and Splice Plate, in terms of determining the fatigue life of the AVLB.
- Depending on the critical crack size of the component, a fracture analysis may be a more or less conservative estimate of fatigue life for the AVLB.
- The fatigue lives of the Hinge and Top Chord are affected substantially by the presence of a crack. Because of this, more focus should be placed on these components during bridge inspections.

- While all components showed a high dependence on initial crack size, the Top Chord and Hinge showed a greater dependence than did the Bottom Chord and Splice Plate, due to their much smaller critical crack sizes.

7. RECOMMENDATIONS

Based on the results of this analysis, the following recommendations and future actions are proposed:

- Test the AVL B to qualify it at MLC 80. This will give actual stress data for the bridge at MLC 80, which can be used to refine the estimate.
- Refine the estimate to reflect 95 percent reliability and confidence (R95C95), as specified for fatigue in [1]. Testing may need to be performed on the materials that comprise the AVL B to obtain the statistical data necessary to adjust the equations used in the analysis to reflect R95C95.
- Verify the results of the analysis. It is recommended that this is done by testing actual hardware. However, a finite element model will suffice, if it can be shown that it represents the actual behavior of the bridge.

ACKNOWLEDGEMENTS

I would like to thank the TARDEC Bridging Team and John Edry of the TARDEC Design Team for their advice and support.

References/ Sources

- 1) Hornbeck, B., Connor, R., Kluck, J., 2005, “Trilateral Design and Test Code for Military Bridging and Gap-Crossing Equipment.”
- 2) Hornbeck, B., 1996, “Addendum to Final Report First Article Test- Government (FAT-G) of the Military Load Class 70 Armored Vehicle Launch Bridge (AVLB),” Test Report, US Army TACOM, Warren, MI.
- 3) Rice, R., Jackson, J., Bakuckas, J., Thompson, S., 2003, “Metallic Material Properties Development and Standardization (MMPDS),” Technical Report No. DOT/FAA/AR-MMPDS-01, Office of Aviation Research, Washington, D.C.
- 4) Lee, Y., Pan, J., Hathaway, R., Barkey, M., 2005, Fatigue Testing and Analysis: Theory and Practice, Elsevier Butterworth-Heinemann, Oxford, UK, Chap. 4-6.
- 5) 2002, “Technical Report on Low Cycle Fatigue Properties Ferrous and Non-Ferrous Materials,” SAE Surface Vehicle Information Report J1099.
- 6) Dowling, N., 1999, Mechanical Behavior of Materials: Engineering Methods for Deformation, Fracture, and Fatigue, 2nd Edition, Prentice Hall, Upper Saddle River, NJ, Chap. 8-11, 14.
- 7) Choi, J., 2000, “The Fracture Analysis and Remaining Life Estimation of the AVLB Sub-Components,” Masters Thesis, West Virginia University, Morgantown, WV.
- 8) ASTM A514/A514M-05. “Standard Specification for High-Yield-Strength, Quenched and Tempered Alloy Steel Plate, Suitable for Welding.
- 9) Sanford, R.J., 2003, Principles of Fracture Mechanics, Pearson Education, Upper Saddle River, NJ, Chap. 2, 9.

Appendix A

AVLB MLC 70 Test Strain Gage Location Drawings

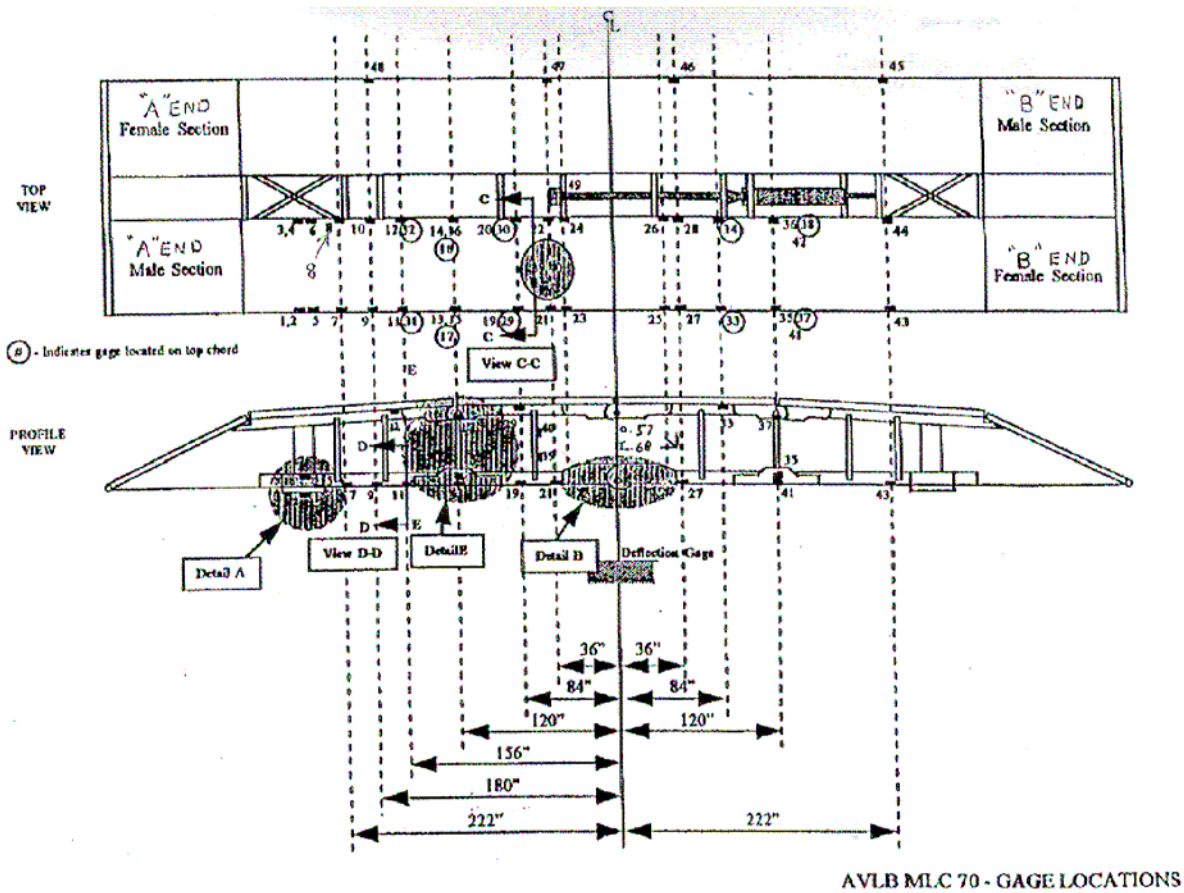


Figure 3: AVLB MLC 70 Test Strain Gage Diagram

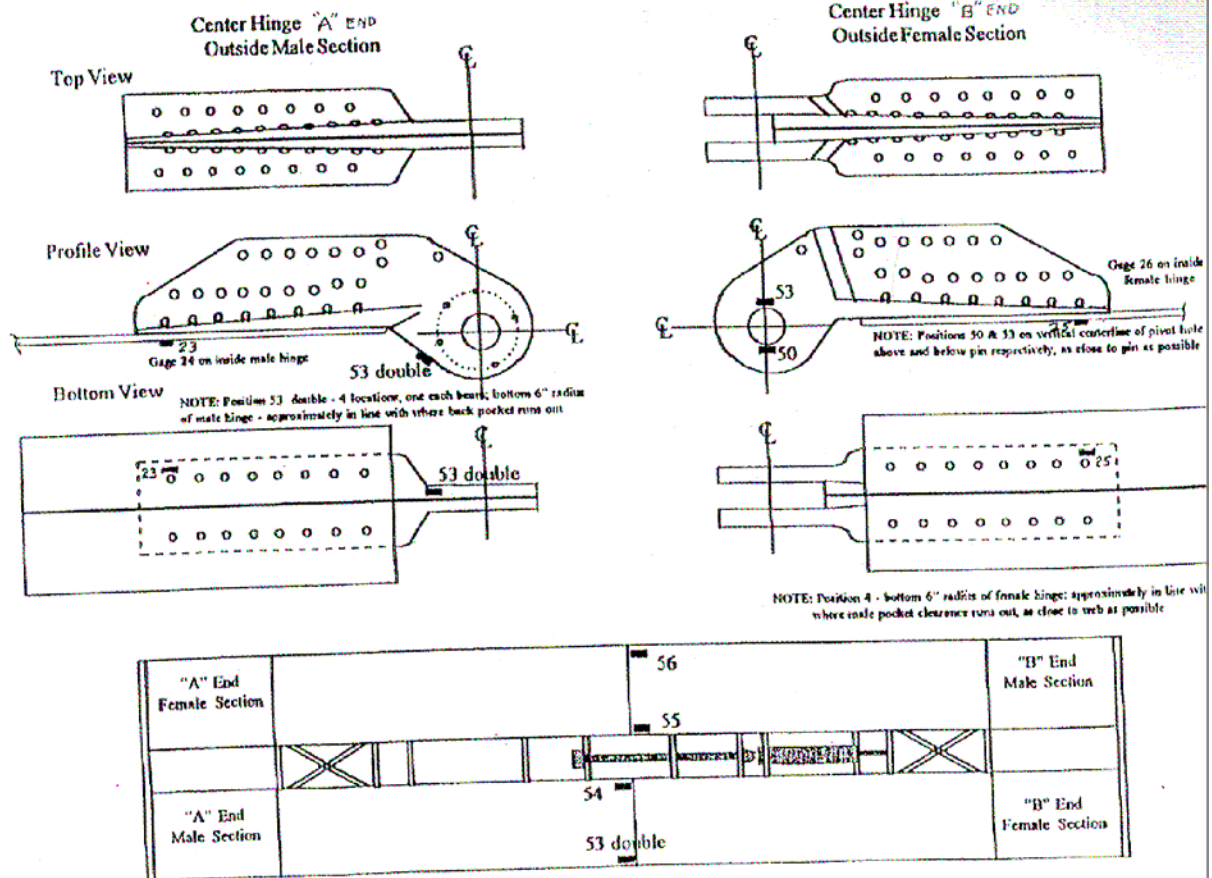


Figure 4: Locations of Strain Gages on Hinge

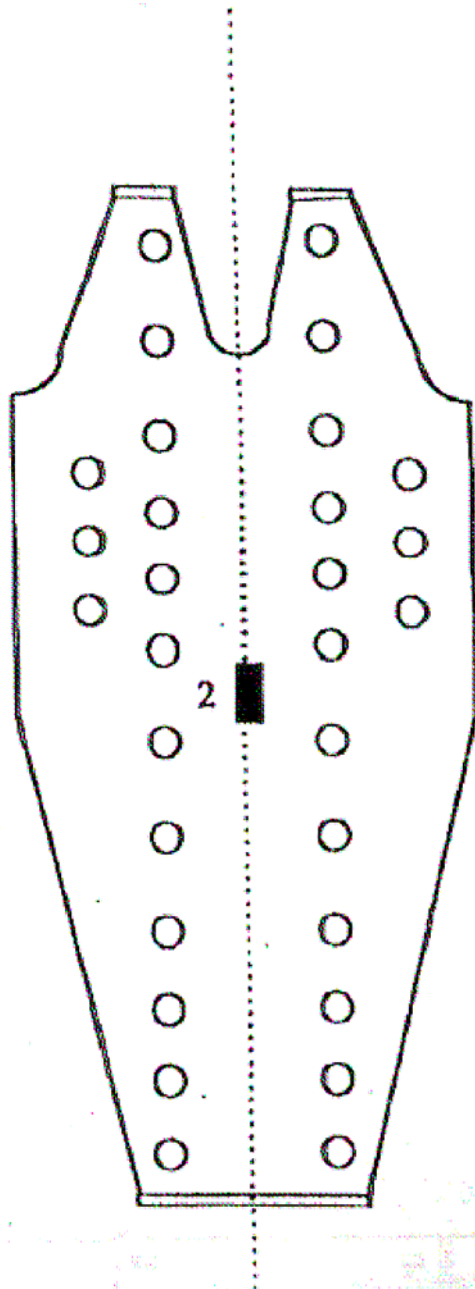


Figure 5: Placement of Strain Gage 2 on Splice Plate

Appendix B

Calculation of T-1 Steel S-N Curve based on Ultimate Strength

T-1 Steel S-N Curve

$$S_u = 800 \text{ MPa} = 116.03 \text{ ksi}$$

$$S_e = 0.5 S_u = 0.5 (116.03 \text{ ksi}) = 58.02 \text{ ksi}$$

$$S_{e0} = 0.9 S_e = 0.9 (116.03 \text{ ksi}) = 104.4 \text{ ksi}$$

Correction Factors

$$C_s = 1.0 \text{ (R50)}$$

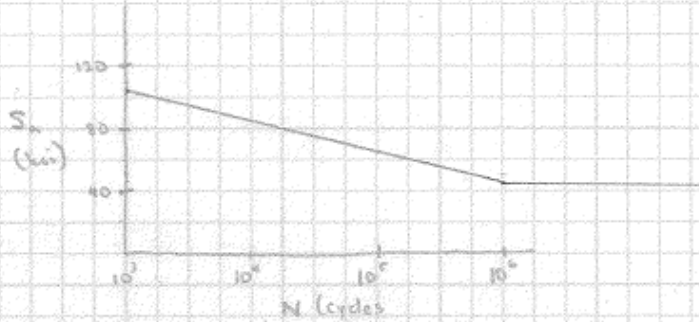
$$C_L = 1.0 \text{ (bending)}$$

$$C_D = 0.75 \text{ (machined, } S_u = 800 \text{ MPa)}$$

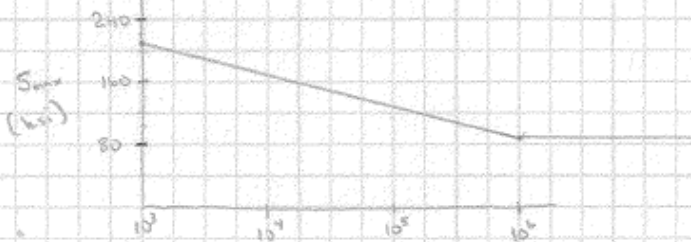
$$C_P = 1 \text{ (Simplification for complex geometry of pt.; assumes } d_c < 8 \text{ mm)}$$

$$S_e = S_{e0} C_s C_L C_D C_P = 0.5 (116.03 \text{ ksi}) (1.0) (1.0) (0.75) \\ \approx 43 \text{ ksi}$$

$$S_{1000, R} = S_{e0} C_s \approx 104 \text{ ksi}$$



$$S_n = \frac{S_{max} - S_{min}}{2} \quad S_{max} = 2S_n$$



$$\log(N_f) = - \left[\left(\frac{\log(10^3) - \log(10^6)}{\log(208) - \log(86)} \right) (\log(208) - \log(S_n)) - \log(10^3) \right]$$

$$\log(N_f) = - \left[-7.8214 [\log(208) - \log(S_n)] - \log(10^3) \right]$$

$$\log(N_f) \approx - \left[-7.8214 \log(S_n) - 7.8214 \log(208) - \log(10^3) \right]$$

$$\log(N_f) \approx -7.8214 \log(S_n) + 21.1304$$